

Proposal to PAC 53

Final-State Interactions Studies in Deuterium at Very High Missing Momenta

C. Yero * [†]

The Catholic University of America, DC

W. Boeglin[†], **M. Sargsian**[‡]

Florida International University, FL

M. Jones[†]

Thomas Jefferson National Accelerator Facility, VA

April 28, 2025

*Contact: yero@cua.edu

[†]Spokesperson

[‡]Theory Collaborator

Executive Summary

One of the most fundamental problems in nuclear physics is to describe the strong nuclear force between protons and neutrons (nucleons) from first principles using Quantum Chromodynamics (QCD) — the fundamental nuclear theory of strong interactions. Understanding the high-momentum structure of the neutron-proton (np) bound system is highly important for nuclear physics due to the observed dominance of short-range correlations (SRCs) in nuclei at nucleon momenta above $\sim 250 - 300$ MeV/ c (Fermi momentum). However, to understand the repulsive part of the NN interaction in $A > 2$ bound systems, one must first understand the simplest ($A = 2$) case without added complications that come with many-body nuclear systems. In addition, a solid understanding of final-state interactions (FSI) and how to suppress them is also required as these interactions distort the reconstruction of the internal relative momenta (\vec{p}_i) of the detected nucleon causing any information about the internal structure of the nucleus to be misinterpreted.

The first high-momentum transfer ($Q^2 > 1$ (GeV/ c)²) studies on the deuteron carried out at Jefferson Lab during the 6-GeV era showed a strong angular dependence of FSI with respect to the neutron recoil angle relative to the momentum transferred (θ_{nq}) where FSI were found to be the strongest at $\theta_{nq} \sim 70^\circ$, while being significantly reduced at forward angles, $\theta_{nq} \sim 30 - 40^\circ$ for neutron recoil (“missing”) momenta up to $p_m \sim 550$ MeV/ c . However, no data that studies this angular dependence currently exists above $p_m \sim 550$ MeV/ c , a kinematic region where the nucleons are expected to significantly overlap and a transition from nucleonic to quark-gluon description of the nucleus is predicted to occur. Therefore, it becomes crucial to have a solid understanding of FSI at very high missing momenta.

We propose to measure the exclusive unpolarized electro-disintegration of the deuteron in Hall C with a 10.55-GeV electron beam incident on a 10-cm long liquid deuterium target. The scattered electrons will be detected by the Super High Momentum Spectrometer (SHMS) in coincidence with the knocked-out protons detected by the High Momentum Spectrometer (HMS), and the recoil (“missing”) neutrons will be reconstructed from momentum conservation. We will focus on the high missing momentum region of $p_m = 800$ MeV/ c and measure the unpolarized absolute cross sections for three central recoil angles: $\theta_{nq} = 49^\circ, 60^\circ, 72^\circ$ at $Q^2 = 4.5$ (GeV/ c)². To extract the angular distributions, a ratio of data cross-sections to a theoretical model of the plane-wave impulse approximation (PWIA) will be taken for a range of recoil angles. This will allow us to precisely determine recoil angles at which FSI are large (or small). To compare the data to theory angular distributions, the cross-section ratio of FSI/PWIA will also be taken for different deuteron theoretical calculations using either the CD-Bonn, AV18 or Paris NN potentials.

This experiment was initially proposed to the Program Advisory Committee PAC 52 as the Letter-of-Intent LOI 12-24-005 (see the Appendix for our response to the questions raised in the PAC 52 comments). We request a total of 548 hrs (23 PAC days) which consists of 540 hrs of physics production and 8 hrs reserved for overhead. This work will complement and contribute to the recent ongoing efforts to explore the elusive deuteron repulsive core, a topic of high theoretical interest motivated by the discrepancy between theory and our recent experimental results in a kinematic region where a transition from nucleonic to quark-gluon description of matter is expected to occur.

Contents

1	Motivation	4
2	Experimental Program	9
3	Proposed measurement	11
3.1	Experimental Method	11
3.2	Simulations	12
3.2.1	Kinematics	14
3.2.2	Acceptance	17
3.3	Projected results	18
3.4	Systematic Uncertainties	21
4	Run Plan	22
5	Summary	23
6	Appendix	26
6.1	PAC 52: LOI 12-24-005 Reader Comments	26
6.1.1	Question:	27
6.1.2	Question:	27

1 Motivation

The deuteron is the most simple bound structure in nuclear physics and is therefore the “ideal laboratory” to study the nuclear short-range interaction. More specifically, when protons and neutrons come in close proximity, at extremely short distances ($\sim 10^{-15}$ m), they must experience a very strong repulsive force that keeps normal matter from collapsing. Unfortunately, not much progress has been made with respect to this aspect of the nuclear force from both a theoretical and experimental standpoint. From the experimental aspect, the limitations have been mainly the low incident electron energies used to probe the nucleus as well as the spectrometer capabilities to detect such high energies. From the theoretical standpoint, since the construction of most nucleon-nucleon (NN) interaction models rely in part in experimental NN scattering data used to constrain the models, a significant advancement in the understanding of the nuclear core has been restricted.

The most direct way to probe the repulsive core of the deuteron np bound-state is via the exclusive $d(e, e'p)$ reaction (see Fig.5). Since the deuteron is a two-body system, we can identify its final state precisely (hence, *exclusive*) and select kinematics to emphasize quasi-elastic knockout of the proton (referred to as plane-wave impulse approximation or PWIA) without competing processes such as (i) neutron-proton re-scattering effects also referred to as final-state interactions (FSI), (ii) meson-exchange currents (MEC) where the virtual photon couples to the exchanged meson or (iii) nuclear excitation into a resonance state (isobar currents or IC), each of which would distort the relationship between the neutron recoil (“missing”) momentum, p_m , and the proton initial momentum, p_i . The relative internal momentum of the bound proton can then be inferred from the reconstructed p_m .

Previous deuteron electro-disintegration experiments carried out at $Q^2 < 1$ (GeV/c)² (see Sec.5 of Ref. [1]) have helped quantify the contributions from FSI, MEC and IC to the $d(e, e'p)$ cross sections and determine kinematics at which these processes are either suppressed (MECs and ICs) or under control (FSI). At larger Q^2 , MEC and IC are expected to be suppressed at $Q^2 > 1$ (GeV/c)², and by selecting Bjorken $x_{Bj} \equiv Q^2/2M_p\nu > 1$ (M_p is the proton mass and ν is the energy transferred) where the lower energy transferred (ν) part of the quasielastic peak is maximally away from the inelastic resonance production threshold. Even at $Q^2 > 1$ (GeV/c)² and $p_m \gtrsim 300$ MeV/c however, FSI are still the dominant contribution to the cross sections compared to the PWIA, therefore they must be studied more carefully.

Final-state interactions have been studied theoretically by several groups [2–9]. In particular, one of the most important results of these studies is described by the generalized eikonal approximation (GEA) initially developed in Refs. [3, 4]. The establishment of the eikonal regime at $Q^2 > 1$ (GeV/c)² is characterized by a very anisotropic angular distribution of the neutron recoil angles relative to the 3-momentum transfers, θ_{nq} , and it makes it possible to identify kinematics where FSI are mostly cancelled (see Fig.1).

The conventional non-relativistic Glauber approximation [4, 10, 11], which considers the bound nucleons as stationary scatterers, predicts FSI to peak at $\theta_{nq} \sim 90^\circ$. The GEA, however, which accounts for relativistic effects, predicts FSI to peak at $\theta_{nq} \sim 70^\circ$ for $p_m \sim 500$ MeV/c. This prediction was confirmed by the first set of high- Q^2 deuteron electro-disintegration experiments carried out at Jefferson Lab [12, 13] (see Fig. 2). Additionally, it was also found that at very forward and backward neutron recoil angles of $\theta_{nq} \sim 40^\circ, 120^\circ$

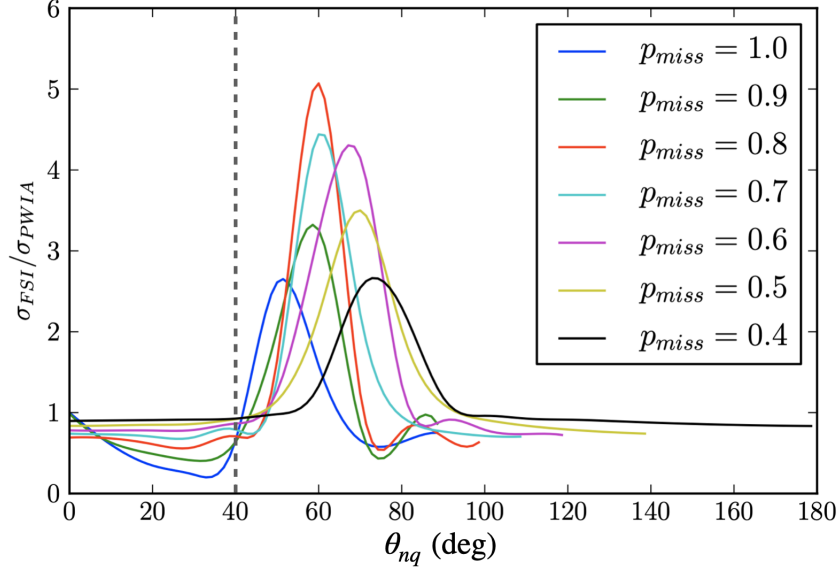


Figure 1: Ratios of the calculated FSI to PWIA cross sections (using the CD-Bonn potential) for different missing momenta as a function of the neutron recoil angle. Note: Reprinted from Ref. [1].

FSI were significantly reduced and comparable to the PWIA. The reduction in FSI can be understood from the fact in the high energy limit ($Q^2 > 1 \text{ (GeV/c)}^2$) of the GEA, the np re-scattering amplitude is mostly imaginary:

$$A = A_{\text{PWIA}} + iA_{\text{FSI}}, \quad (1)$$

with $A_{\text{FSI}} \approx i|A_{\text{FSI}}|$, where the total scattering amplitude A is expressed as the sum of the PWIA (A_{PWIA}) and the imaginary part of the FSI (A_{FSI}) scattering amplitudes. The total theoretical cross section can then be obtained by taking the modulus square of the total scattering amplitude and can be expressed as

$$\sigma_{\text{FSI}} \sim |A|^2 = |A_{\text{PWIA}}|^2 - 2 \underbrace{|A_{\text{PWIA}}||A_{\text{FSI}}|}_{\text{"Screening" or interference term}} + \underbrace{|A_{\text{FSI}}|^2}_{\text{re-scattering term}}. \quad (2)$$

Taking the ratio of the total to the PWIA part of the cross section,

$$R = \frac{\sigma_{\text{FSI}}}{\sigma_{\text{PWIA}}} = 1 - 2 \frac{|A_{\text{PWIA}}||A_{\text{FSI}}|}{|A_{\text{PWIA}}|^2} + \frac{|A_{\text{FSI}}|^2}{|A_{\text{PWIA}}|^2}. \quad (3)$$

From the ratio of cross sections the interference term enters with an opposite sign as compared to the re-scattering term, which provides an opportunity for an approximate cancellation at certain neutron recoil angles as shown in Figs. 1 and 2. This cancellation is also approximately independent of the neutron recoil momenta, which opens a kinematic window at $\theta_{nq} \sim 40^\circ$ where one can probe the short-range structure of the deuteron beyond $p_m \sim 500 \text{ MeV/c}$.

Another important feature of the GEA, and perhaps the one most relevant to this proposal is that the FSI peak, originally at $\theta_{nq} \sim 70^\circ$ for $p_m = 0.5$ GeV/c, shifts toward smaller recoil angles with increasing missing momenta as shown in Fig.1. This raises a very important question regarding the experimental sensitivity of the high-momentum component of the deuteron to FSI. In the most recent deuteron electro-disintegration experiment at Hall C [14], the internal momentum probed was extended up to $p_m \sim 940$ MeV/c (see Fig.3) at kinematics optimized for reducing FSI, based on the results from Ref. [12] (see Fig.2), by selecting central recoil angles $\theta_{nq} \sim 40^\circ$.

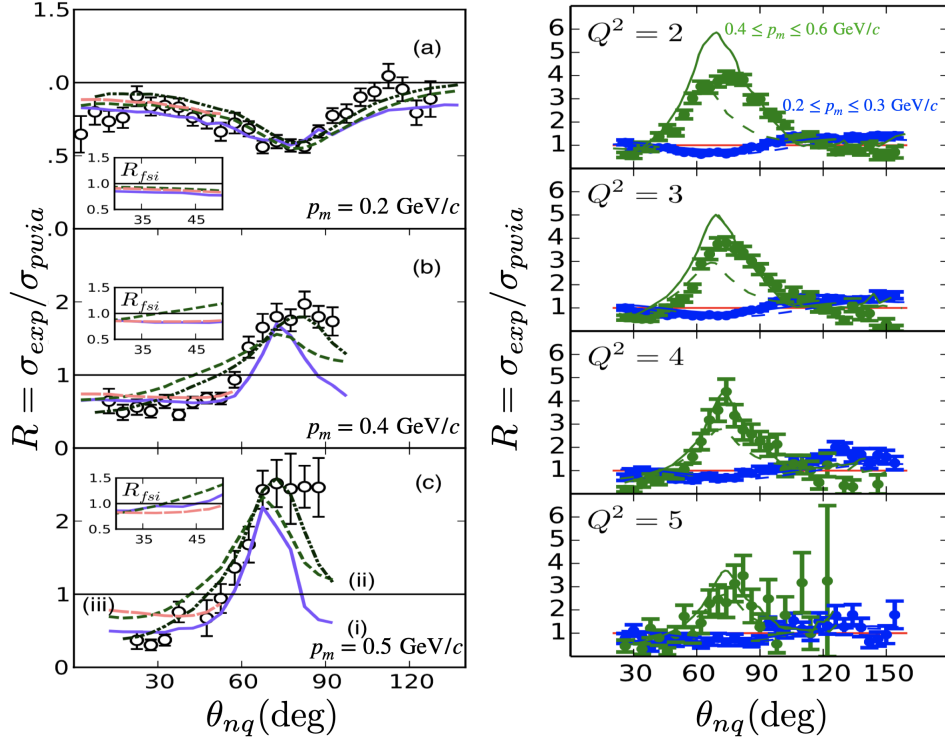


Figure 2: $^2\text{H}(e, e'p)n$ angular distributions of the cross section ratio, $R = \sigma_{exp}/\sigma_{pwia}$. (Left) Hall A data at $Q^2 = 3.5 \pm 0.25$ (GeV/c)² and missing momentum settings (a) $p_m = 0.2$ GeV/c, (b) $p_m = 0.4$ GeV/c and (c) $p_m = 0.5$ GeV/c. Theoretical calculations for (i) solid (purple) curves using the CD-Bonn potential by M. Sargsian [8], (ii) dashed (green) curves using FSI and dashed-double dotted (black) curves using FSI+MEC+IC by J.M. Laget [6] using the Paris potential and (iii) dashed (pink) curves denote calculations by J.W. Van Orden [7]. (Right) Hall B data at various Q^2 settings. The green data (with FSI re-scattering peak) correspond to $400 \leq p_m \leq 600$ MeV/c, and the blue data (no FSI re-scattering) correspond to $200 \leq p_m \leq 300$ MeV/c. The solid curves are calculations from J.M. Laget [6] and the dashed curves are from M. Sargsian [8]. Note: Reprinted from Ref. [1].

As shown in Fig.3, the data agrees well with the previous Hall A measurements [12] and is reproduced by all non-relativistic deuteron calculations for missing momenta up to $p_m \sim 550$ MeV/c, however, **no theoretical model reproduces the data above $p_m \sim 750$ MeV/c**. It is also interesting to note that recent theoretical calculations by Sargsian & Vera [15] (see Fig.4) using a relativistic deuteron wavefunction start to significantly deviate from

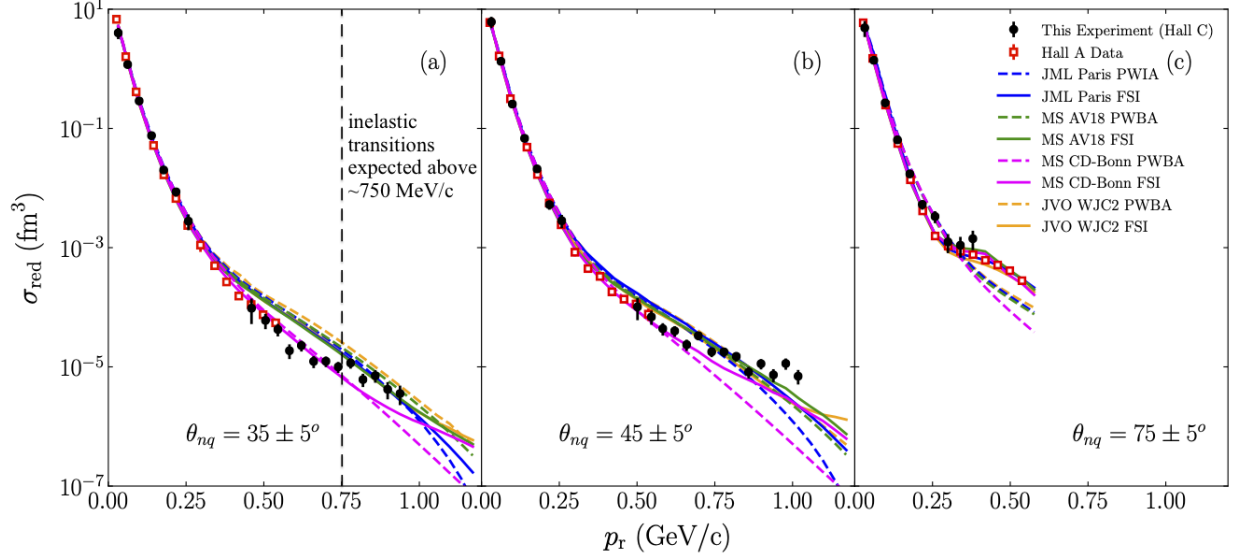


Figure 3: The experimental reduced cross sections (momentum distributions) for three values of the recoil angle θ_{nq} at $Q^2 = 4.5 \pm 0.5$ (GeV/c)² [14]. The solid lines are calculations including FSI and the dashed lines correspond to PWIA calculations [8].

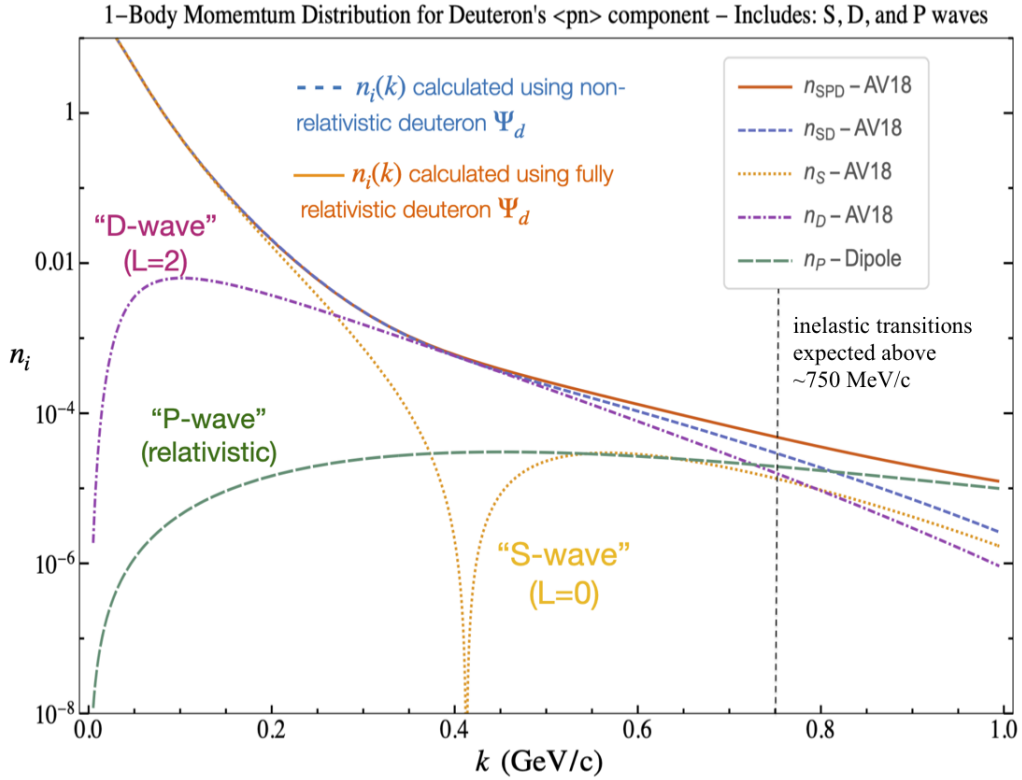


Figure 4: 1-body Momentum Distributions of the Deuteron using the AV18 potential. Reprinted from Ref. [16]

the non-relativistic calculations precisely at internal momenta ~ 750 MeV/c which coincides with our published results (see Fig.3) from Ref. [14]. This disagreement can be attributed to an enhanced role of the relativistic effects at higher internal momenta. At such extreme momenta, inelastic transitions such as $\Delta\Delta \rightarrow np$ or $NN^* \rightarrow np$ (Δ and N^* denote Δ -isobar and N^* resonances) corresponding to the non-nucleonic components of the deuteron are expected to appear in the deuteron wavefunction. The similarities observed between our data and the recent relativistic deuteron calculations could be a possible indication of the onset of non-nucleonic degrees of freedom given that $p_m \sim 750$ MeV/c corresponds to the inelastic threshold in the np channel [15].

Furthermore, from Fig.3 it is interesting to note that the onset of FSI (solid magenta for CD-Bonn calculations) starts already at $p_m \sim 800$ MeV/c for $\theta_{nq} = 35 \pm 5^\circ$, and as early as $p_m \sim 600$ MeV/c for $\theta_{nq} = 45 \pm 5^\circ$. It is therefore crucial to be able to experimentally verify whether or not any potential contributions from FSI exist at very high missing momenta. If it is found that FSI do not contribute to the observed discrepancy between data and theory calculations (see Fig.3), then this proposed experiment could open up the possibility for a dedicated study of one of the most outstanding issues in nuclear physics— understanding the dynamics of a transition between hadronic to quark-gluon phases of matter.

In this experimental proposal, our objective is to extend the angular distributions measured in Ref. [12] (see Fig.2 (left)) to a central missing momentum of $p_m = 800$ MeV/c, a critical region corresponding to the repulsive core around which none of the deuteron models is able to reproduce the data in Fig.3. The proposed measurement will enable us to determine more precisely, the kinematic region where FSI are reduced, as well as separate the effects of FSI from possible contributions of non-nucleonic components of the deuteron [15], which are expected to show up around $p_m \sim 750$ MeV/c.

2 Experimental Program

We propose to measure the $d(e, e'p)n$ absolute cross sections at $Q^2 = 4.5 \pm 0.5 \text{ (GeV/c)}^2$ for 3 central recoil angles: $\theta_{nq} = 49^\circ, 60^\circ, 72^\circ$ corresponding to a central missing momentum setting of $p_m = 800 \text{ MeV/c}$. The selected recoil angles will provide a wide angular coverage to map out the FSI dependence on θ_{nq} . The angular distributions will be extracted by taking the ratio of the experimental cross sections to the PWIA theoretical cross sections versus neutron recoil angles, θ_{rq} . At such high Q^2 , it is expected that MEC and IC will have negligible contributions to the experimental cross sections for forward recoil angles. At larger angles ($\theta_{nq} > 70^\circ$), where $x_{Bj} < 1$, however, IC can still contribute significantly due to being near the inelastic electroproduction threshold, as evidenced by the data points in the last panel in Fig.2(left).

Measurements will also be done at $p_m = 500 \text{ MeV/c}$ for $\theta_{nq} = 70^\circ$ at the same Q^2 . These data will be used for normalization measurements and comparison to the Hall A data [12]. In addition, we will also measure the $^1\text{H}(e, e'p)$ hydrogen elastic reaction to (i) check the spectrometer acceptance models, (ii) study target boiling effects and (iii) check systematic effects on beam energy and the spectrometer' central momentum and angle.

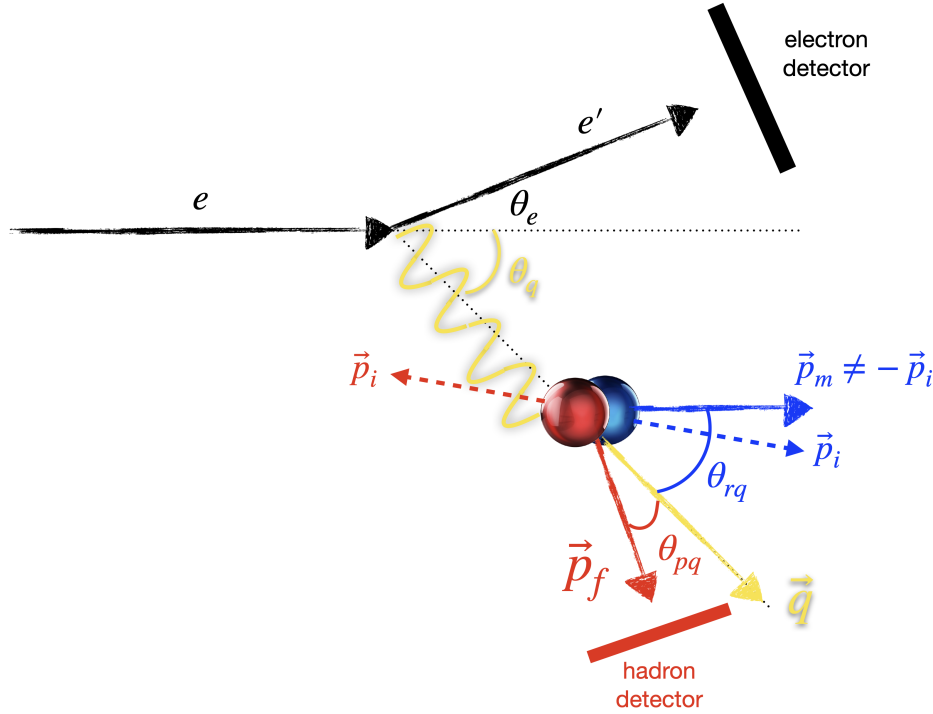


Figure 5: Schematic diagram of the $d(e, e'p)n$ reaction.

The experiment will be carried out at Jefferson Lab Experimental Hall C. A 10.55-GeV, $3 \times 3 \text{ mm}^2$ square-rastered electron beam will be incident on a 10-cm long liquid deuterium target. A typical $d(e, e'p)n$ reaction is shown in Fig.5 in which the incident electron interacts with the deuteron via the one-photon exchange approximation (OPEA), in which the scattered electron (k_f, θ_e) is detected by the Super High Momentum Spectrometer (SHMS) in coincidence with the knocked-out proton (p_f, θ_p) detected by the High Momentum Spectrometer

(HMS). The recoil neutron momenta (p_m) is reconstructed from momentum conservation. In Fig.5, the dashed vectors represent the relative internal momenta of the bound nucleons before interacting with the virtual photon. After the interaction, the bound proton is directly knocked-out, modifying its momentum. Within the PWIA, the spectator neutron would recoil with a missing momentum $\vec{p}_m = -\vec{p}_i$. However, due to FSI, the neutron re-interacts with the proton causing a modification in its recoil momentum such that $\vec{p}_m \neq -\vec{p}_i$. The modification of the neutron recoil momentum by FSI destroys any information related to the internal momentum of the deuteron. In either case, the modified missing momentum is determined by the vector difference $\vec{p}_m = \vec{q} - \vec{p}_f$, as show in Fig.6. The central spectrometer kinematics are summarized in Table 1. A detailed description of the kinematics is covered in Section3.2.1.

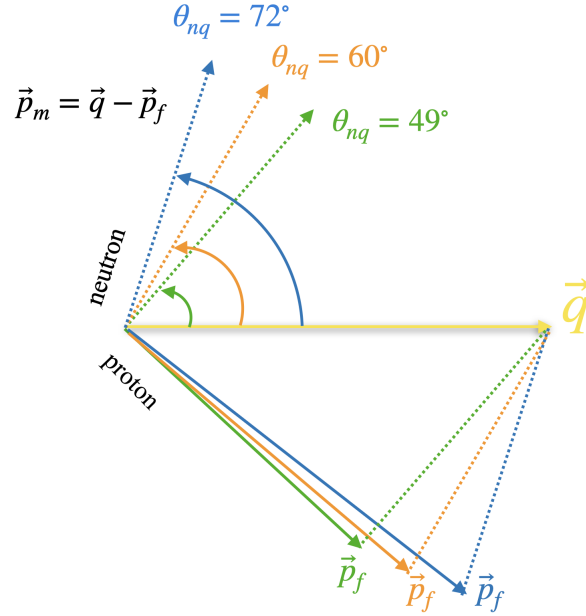


Figure 6: Schematic diagram showing the vector reconstruction of the recoil neutron \vec{p}_m from the virtual photon momentum transferred, \vec{q} , detected proton, p_f for each of the three central recoil angles, θ_{nq} . The dashed lines at the proton side are for reference.

p_m (MeV/c)	θ_{nq} (deg)	k_f (GeV/c)	θ_e (deg)	p_f (GeV/c)	θ_p (deg)
500	70	8.151	13.14	3.069	44.17
800	49	8.551	12.82	2.468	54.85
	60	8.151	13.14	2.891	49.27
	72	7.552	13.65	3.516	41.57

Table 1: Central spectrometer kinematics coverage for an incident electron beam energy of $E_b = 10.55$ GeV and $Q^2 = 4.5$ (GeV/c) 2 .

3 Proposed measurement

In the following section we describe the experimental observable, the expected kinematic coverage from simulations and the expected results.

3.1 Experimental Method

Within the PWIA, the virtual photon couples directly to the bound proton, which is subsequently ejected from the deuteron without any further interaction with the recoiling neutron, the neutron carries a momentum equal in magnitude but opposite in direction to the initial momentum of the bound proton, $\vec{p}_m = -\vec{p}_i$, thus providing information on the momentum of the bound proton and its momentum distribution. However, if FSI are accounted for, the neutron momentum is modified by re-scattering with the knocked-out proton, and $\vec{p}_m \neq -\vec{p}_i$. For this specific case, assuming IC and MEC are negligible, one can still factorize the differential cross-section as follows:

$$\frac{d^6\sigma}{dE'd\Omega_e d\Omega_p dT_p} = K \cdot \sigma_{eN} \cdot S_D(\vec{p}_m \neq \vec{p}_i, E_m), \quad (4)$$

where K is a kinematic factor and σ_{eN} describes the elementary cross section for an electron scattering off a bound (off-shell) nucleon where the deForest [17] off-shell cross sections, σ_{cc1} or σ_{cc2} , are commonly used. The $S_D(\vec{p}_m, E_m)$ is referred to as a “distorted” spectral function, due to the modification of the recoil neutron momentum. In the approximation of $p_m \sim p_i$ (PWIA), the spectral function $S(\vec{p}_m \approx \vec{p}_i, E_m)$ would otherwise describes the probability of finding a bound proton with momentum \vec{p}_i and separation (“missing”) energy E_m .

We use the standard definition of missing energy: $E_{\text{miss}} = \nu - T_p - T_{\text{rec}}$, where ν is the energy transferred to the nucleus, and (T_p, T_{rec}) are the proton and recoil kinetic energies, respectively. For the special case of a deuteron break-up reaction, the recoil kinetic energy refers to that of the neutron. Since the deuteron has no excited states, the kinetic energies of the proton and neutron are well-defined and the missing energy becomes the binding energy of the deuteron, ~ 2.2 MeV. It follows that for the special case of the deuteron bound state, the separation (binding) energy can be integrated out of Eq. 4 to obtain,

$$\sigma_{\text{theory}} \equiv \frac{d^5\sigma_{\text{theory}}}{dE'd\Omega_e d\Omega_p} = K f_{\text{rec}} \sigma_{eN} S_D(\vec{p}_m), \quad (5)$$

where f_{rec} is the recoil factor that arises from the integration in E_m and is defined as [18]

$$f_{\text{rec}} \equiv \frac{1}{1 - \frac{\frac{1}{2} E_f q^2 - (p_f^2 + p_m^2)}{p_f^2}}. \quad (6)$$

where E_f is the final proton energy and E_r is the final neutron recoil energy (note this is different than E_m). From the experimental side, one can then take the ratio of the experimental cross sections to the theoretical cross sections only within the PWIA and bin the events in θ_{nq} to extract the angular distributions, similarly to the ones shown in Fig.2.

3.2 Simulations

The standard Hall C $A(e, e'p)$ coincidence simulation package (SIMC) was used to estimate the count rates for electron-scattering off a 10-cm long liquid deuterium target. The $d(e, e'p)n$ reaction was simulated for each of the central kinematics described in Table 1. The events were weighted by the theoretical model of the deuteron from J.M. Laget for both PWIA and FSI (Paris NN potential) [6]. Furthermore, an efficiency factor based on the prior deuteron experiment [14] was also applied to the weight in order to account for experimental detector tracking inefficiencies in HMS/SHMS (3% / 4%), data-acquisition dead-time (1%), target boiling effects (5%) and proton absorption (5%), which further reduced the yield in order to have a more conservative estimate.

additional simulation effects:

To have a more realistic estimate of the count rates, (i) *radiative* and (ii) *energy loss* effects were also included in the simulation. Radiative effects can significantly change the electron kinematics and therefore the measured yields. Energy loss effects account for the particles passage through the detector/spectrometer entrance and exit windows which also leads to a measurable effect in the yields.

event-selection cuts:

To select $d(e, e'p)$ coincidence events, we used the standard definition of missing energy in: $E_{\text{miss}} = \nu - T_p - T_{\text{rec}}$ previously defined in Section 3.1. Due to the finite energy resolution of the spectrometers, however, the binding energy of the deuteron is spread about its central value. In addition, spectrometer momentum ($\Delta P/P_0$) and angular acceptance cuts were also applied. The momentum acceptance refers to a relative variation of the detected particle momentum, ΔP , with respect to the spectrometer central momentum, P_0 . The angular acceptance refers to a relative variation in the scattered particles in-plane and out-of-plane angles with respect to the central spectrometer angle. The events are reconstructed and projected back to a collimator where the angular acceptance cut is applied. A summary of the cuts applied is presented in Table 2. The kinematics distributions are shown in 3.2.1.

analysis cut	range
E_{miss}	-20 to 40 MeV
Q^2	4 to 5 (GeV/c) ²
HMS $\Delta P/P_0$	-10 to 10 %
SHMS $\Delta P/P_0$	-10 to 22 %
HMS collimator	octagonal
SHMS collimator	octagonal

Table 2: SIMC event-selection cuts

background contributions:

From the previous $d(e, e'p)n$ coincidence experiment at Hall C [14], it was shown that the background sources were negligible as shown in Fig.7 (left) where the electron singles (SHMS), proton (HMS) singles and coincidence rates. The right panel of that same figure shows a typical coincidence time spectrum for the $p_m = 80$ MeV/c setting. Therefore, we expect that the background contributions and trigger rates will not be a problem for the proposed experiment, which explores a similar region of missing momenta larger recoil angles ($\theta_{nq} \sim 49, 60, 72^\circ$) as compared to $\theta_{nq} \sim 40^\circ$ measured in Ref. [14].

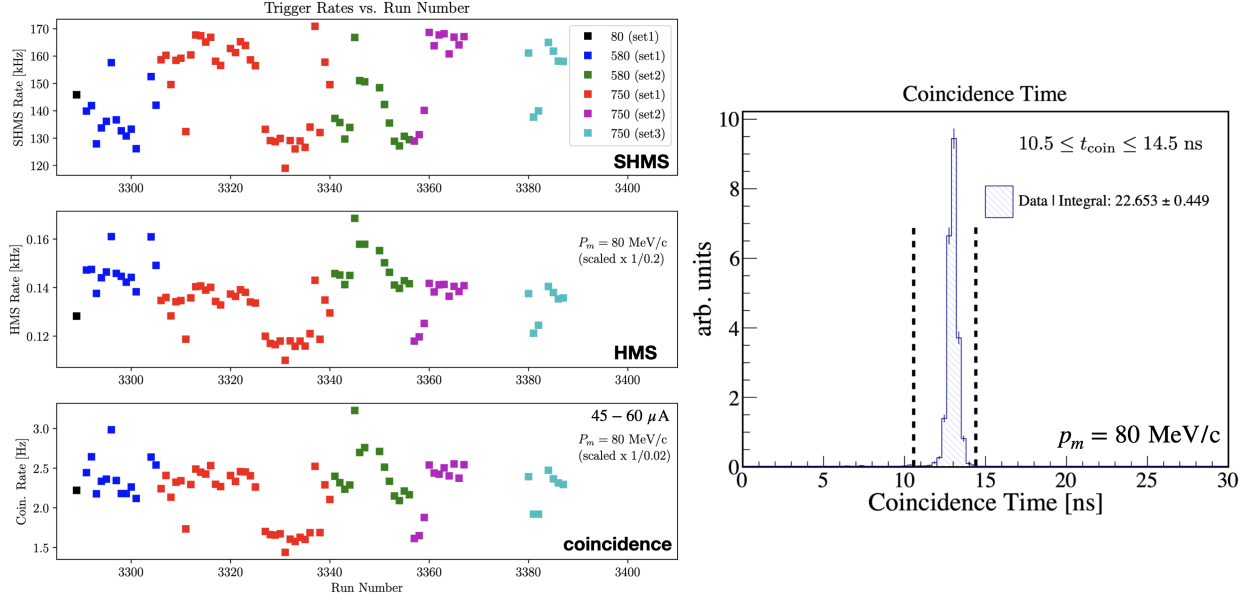


Figure 7: Trigger rates for the SHMS (top, in kHz), HMS (middle, in kHz) and coincidence trigger (bottom, in Hz) during the E12-10-003 experiment. Reprinted from Ref. [19].

count rate estimates:

p_m (MeV/c)	θ_{nq} (deg)	$d(e, e'p)$ rates (counts/hr)	DAQ rates (Hz)	beam-on-target (hrs)
500	70	456	0.467	12
800	49	41	0.0585	200
	60	105	0.101	144
	72	114	0.105	160

Table 3: $d(e, e'p)n$ rate estimates using the Laget FSI model with incident beam energy of 10.55 GeV at 80 μ A. Data-Acquisition (DAQ) rates exclude analysis cuts.

The following subsections show the relevant kinematic and acceptance variables with all event-selection cuts (Table2) and appropriately scaled by the beam-on-target.

3.2.1 Kinematics

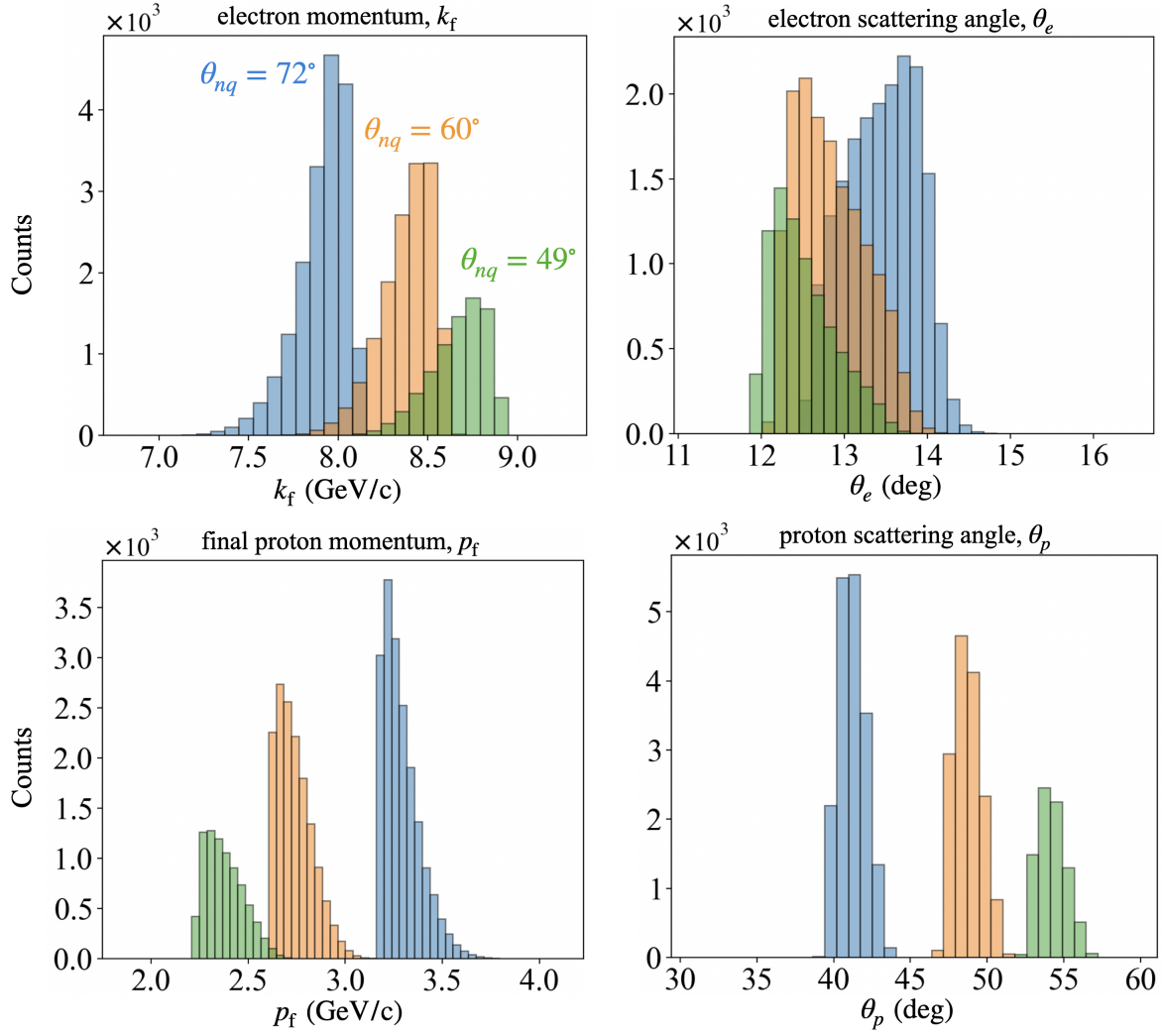


Figure 8: Simulated spectrometer kinematic distributions for SHMS (electrons) and HMS (protons) at 80 μA .

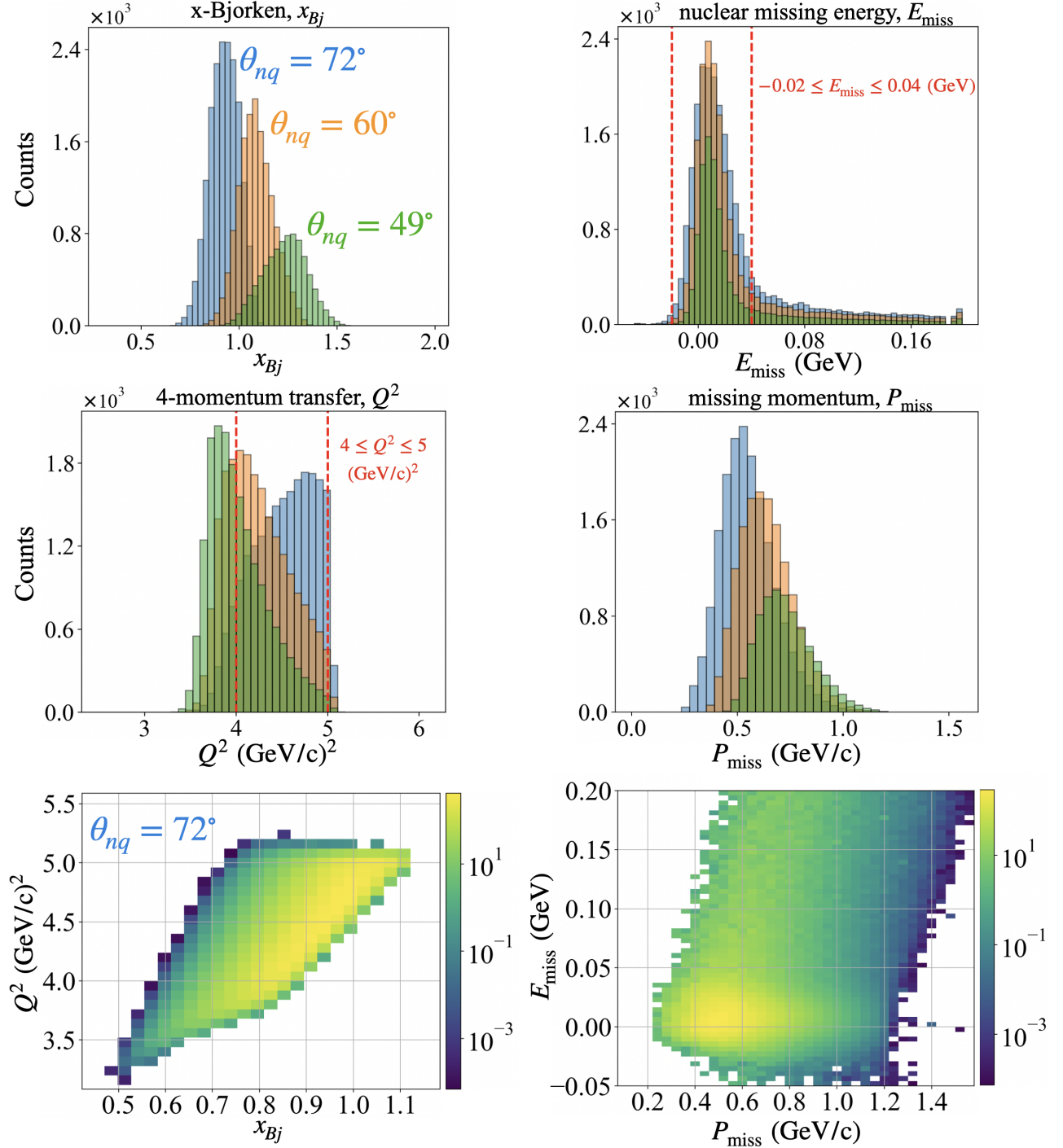


Figure 9: Additional kinematic distributions for x_{Bj} and Q^2 : (bottom 2 panels) 2D correlations of Q^2 vs. x_{Bj} (left) and E_{miss} vs. P_{miss} only for $\theta_{nq} = 72^\circ$. The color bar indicates the counts.

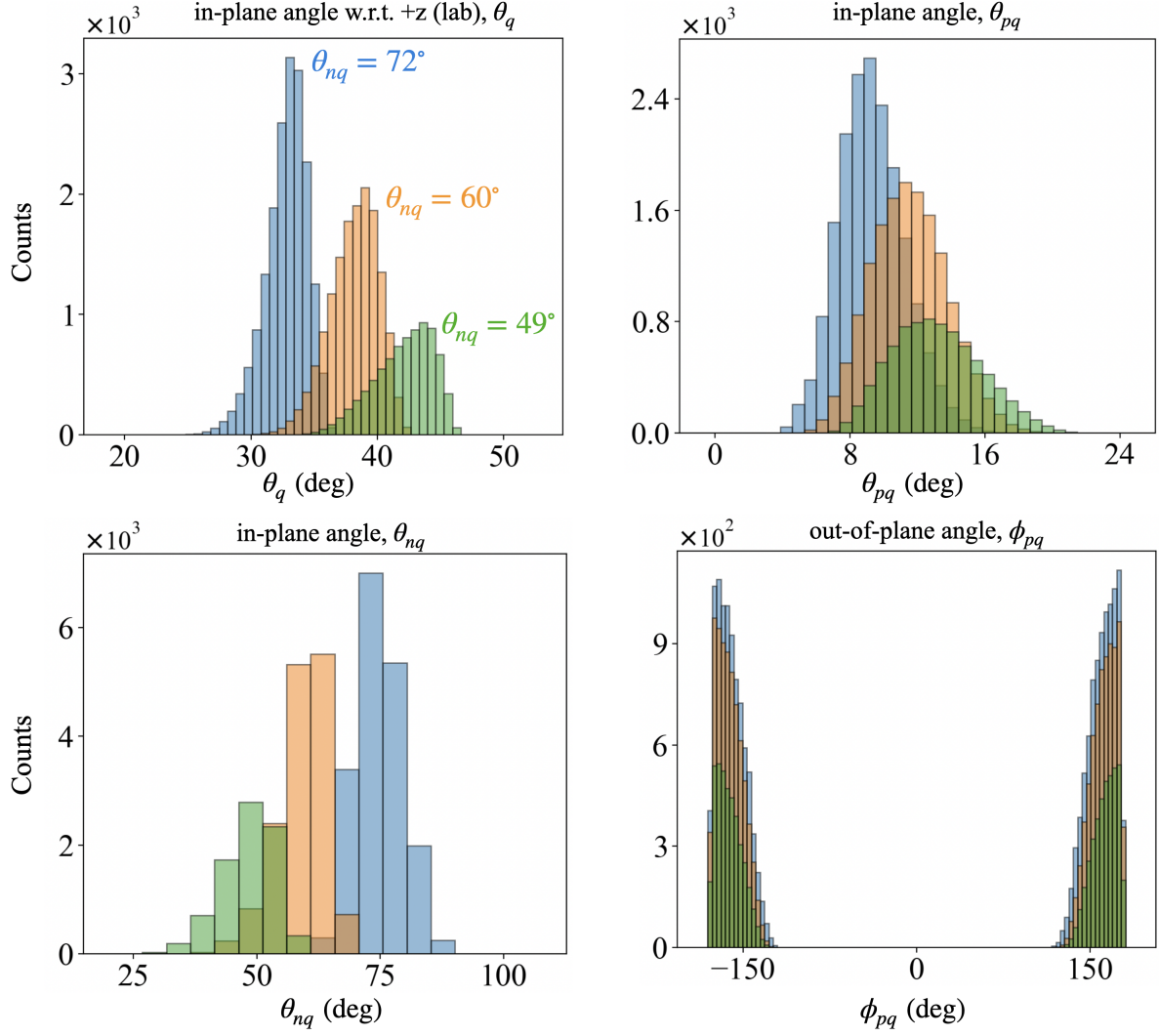


Figure 10: Angular kinematics showing the angles of \vec{q} and the angles of the proton and neutron relative to \vec{q} at 80 μA .

3.2.2 Acceptance

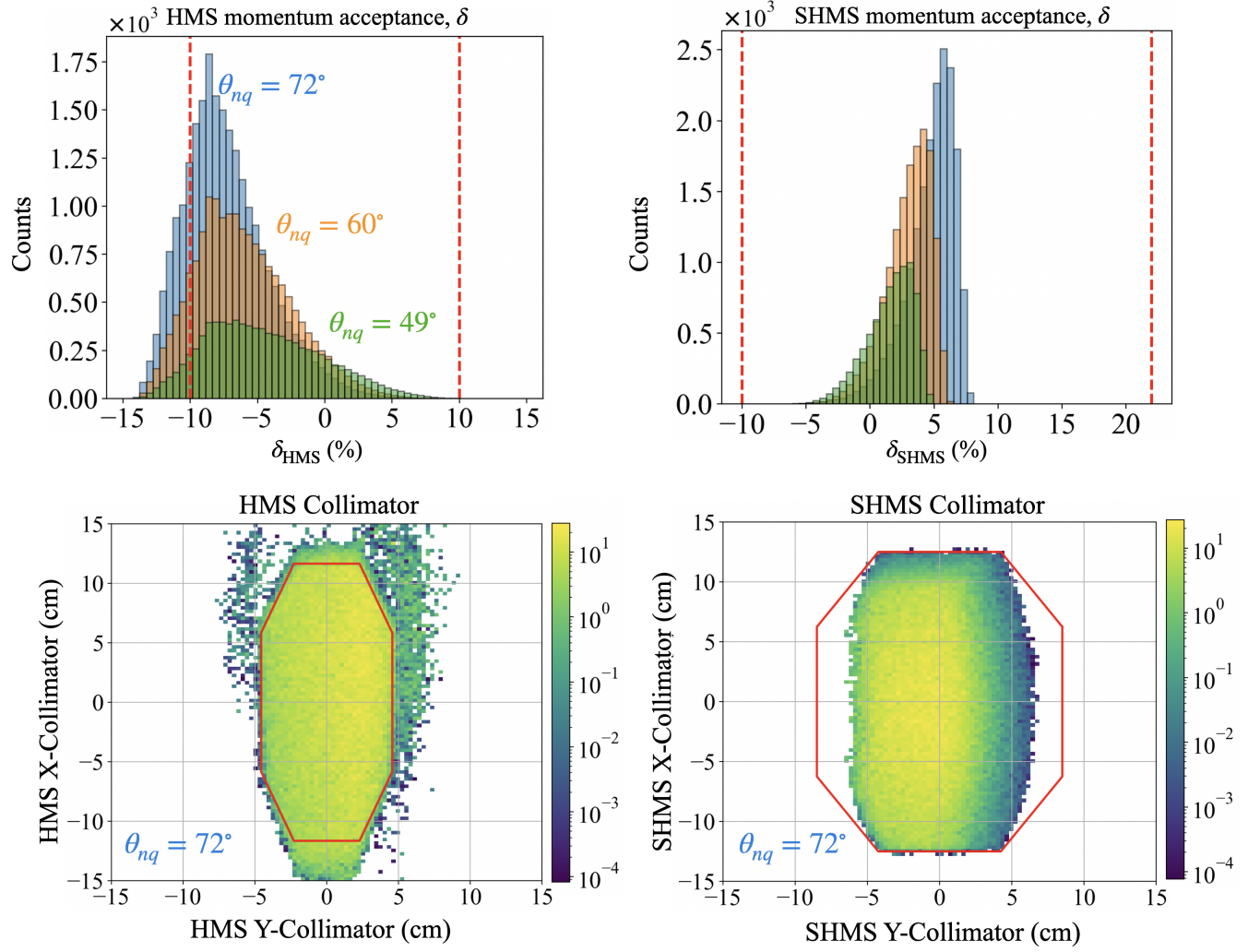


Figure 11: Momentum (top) and angular (bottom) acceptance distributions. The bottom panels show a contour line indicating the collimator geometry boundary; the HMS collimator determine the acceptance of the SHMS, as evidenced by most events in SHMS acceptance falling within the collimator geometry.

3.3 Projected results

The simulation yield for both PWIA and FSI are binned in terms of $(p_{\text{miss}}, \theta_{nq})$ as shown Fig.12(top:FSI, bottom: PWIA). All analysis cuts summarized in Table2 have been applied.

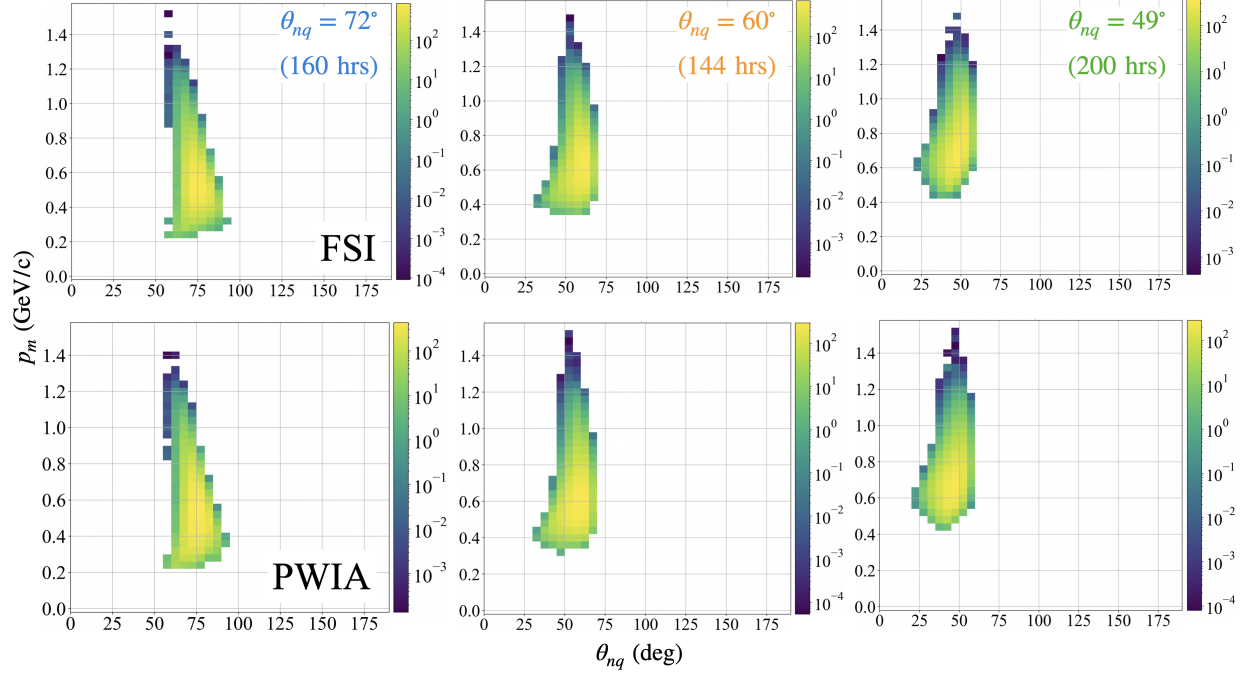


Figure 12: 2D correlation yield of p_{miss} vs. θ_{nq} for $\theta = 49, 60, 72^\circ$ using Laget FSI model [6].

To extract the angular distributions, the ratios of the 2D FSI to PWIA were taken for each (p_m, θ_{nq}) bin presented in Fig.12. The resulting ratio was then plotted versus θ_{nq} for different slices of p_m as shown in Fig.13. From the angular distributions, a FSI peak is clearly visible and starting at $\theta_{nq} = 70^\circ$ in the first p_m bin, and shows a gradual shift towards forward angles. One can also observe that the crossing at $\theta_{nq} \sim 40^\circ$, where the ratio is 1, is consistent throughout all the bins indicating the kinematic region where cancellation between the FSI and the PWIA/FSI interference term occurs, as was discussed earlier. These predictions have been experimentally verified for $p_m < 500$ MeV/c, but will need to be verified for $p_m > 500$ MeV/c, where relativistic effects play a more significant role. Furthermore, theoretical calculations that incorporate a relativistic deuteron wavefunction within the GEA are currently being developed by M. Sargsian using both the CD-Bonn and the AV18 potentials.

Figure 14 shows the projected statistical relative error on the FSI/PWIA ratios from Fig.13, where the red (dashed) lines used as a reference, represent the $\pm 20\%$ relative error mark, showing that most of the data points fall well within a statistical uncertainty of 20%.

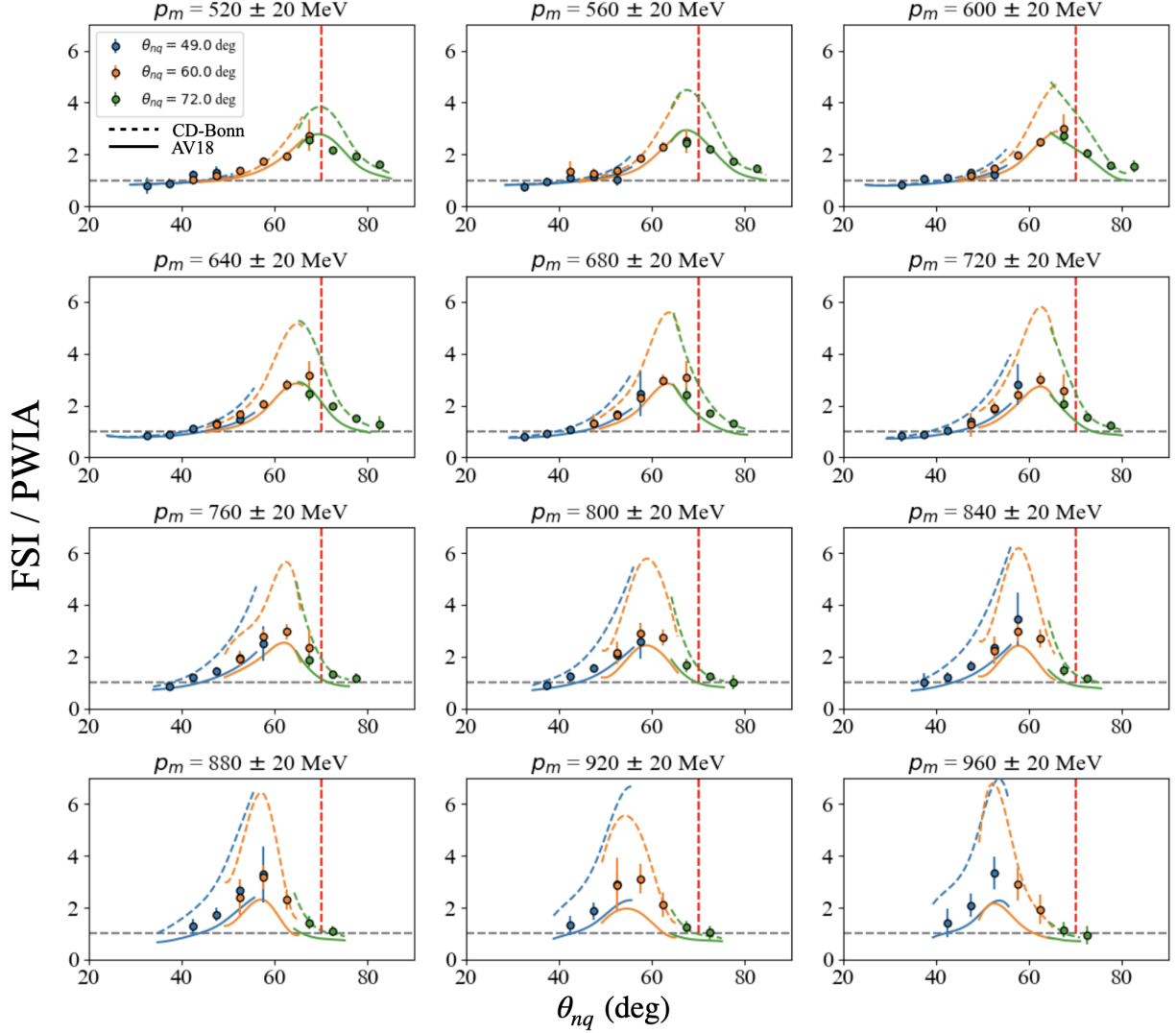


Figure 13: Angular distributions for θ_{nq} for $\theta = 49, 60, 72^\circ$ for a range of p_m bins using the Laget model (circles) of the deuteron. The dashed (CD-Bonn) and solid (AV18) theory curves are calculations within the GEA framework by Sargsian [8]. The dashed (gray) horizontal line at 1 is used as a reference indicating no FSI. The dashed (red) vertical line is placed at $\theta_{nq} = 70^\circ$ for reference, to more easily observe the shift in the FSI peak.

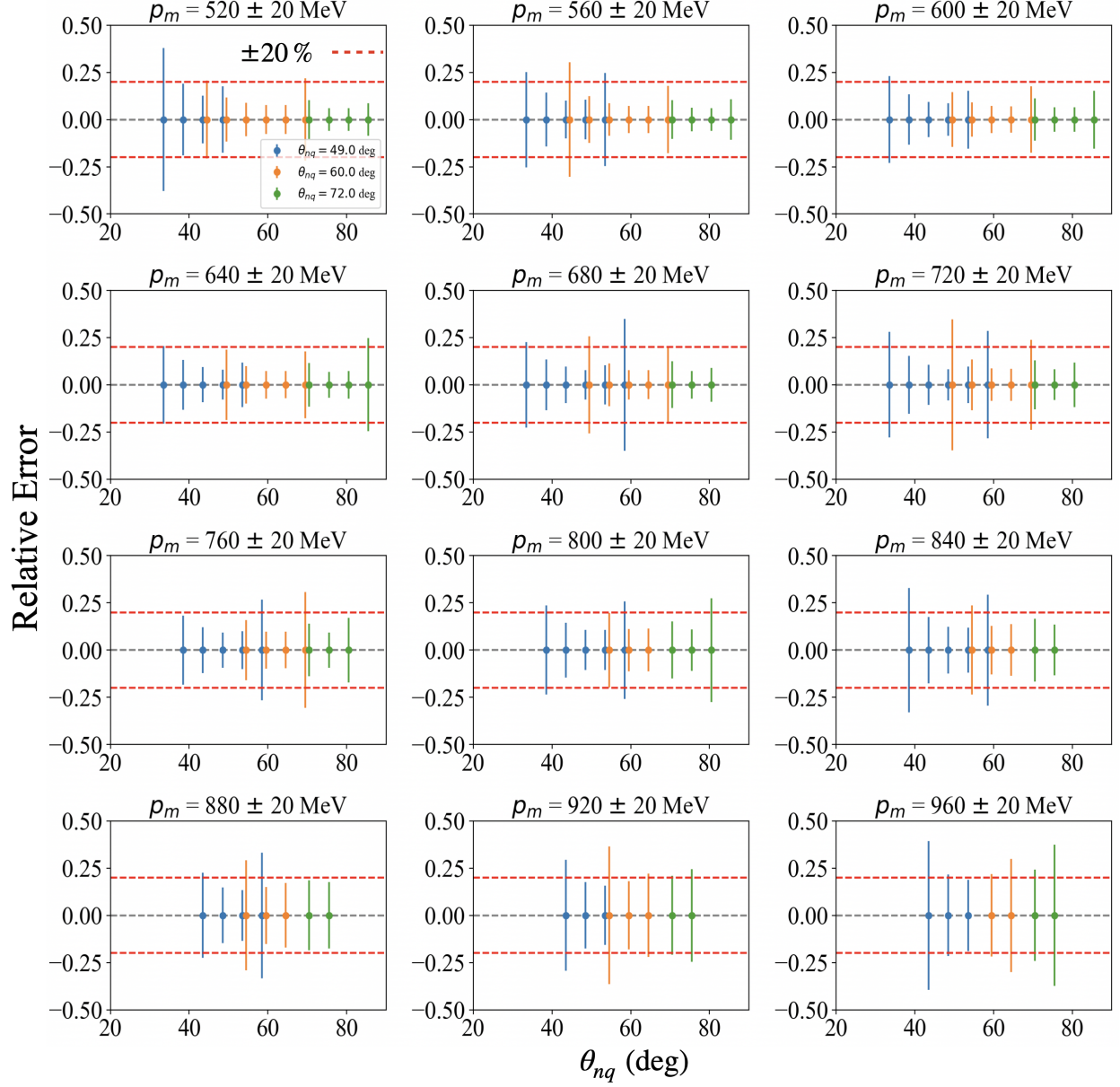


Figure 14: Relative error of angular distributions for θ_{nq} for $\theta = 49, 60, 72^\circ$ for a range of p_m bins using the Laget model of the deuteron. The dashed red lines indicate a $\pm 20\%$ relative error used as a reference.

3.4 Systematic Uncertainties

From the previous $d(e, e'p)$ measurements at Hall C [14, 19], which covered the range of missing momentum as that presented in this proposal, the major source of systematic uncertainties were well below 10%. There are two major sources of systematic uncertainties: (i) normalization, and (ii) kinematics.

The normalization uncertainties were typically on the order of 3 – 4% mainly due to the beam-current monitoring (BCM) calibration used in determining the charge normalization factor, the data acquisition dead time corrections as well as target boiling and proton absorption normalization corrections, as described in Ref. [19].

The kinematics uncertainties come mainly from the uncertainty in the determination of the incident beam energy as well as the spectrometers' momentum and angle settings. These are usually determined by a series of dedicated hydrogen elastic data. From Ref. [14], these uncertainties were determined point-to-point in (p_m, θ_{nq}) bin and were added in quadrature for overlapping bins, with an overall kinematic uncertainty below 6.5%.

Given the similarity between the missing momentum range presented in this proposal and the commissioning deuteron experiment [14], we are confident that the overall systematic uncertainties will not go above 10%.

4 Run Plan

We propose a total of 548 hrs (~ 23 PAC days) with 10.55-GeV beam energy, which consists of 540 hrs of physics production and 8 hrs of overhead. The overhead will be primarily allocated for the spectrometer momentum/angle changes between each of the central settings. Table 4 gives an overview of the time allocations for each part of the experiment.

From past experience on the data analysis of $d(e, e'p)$ at high missing momentum in Hall C [14, 19], we estimate the singles rates of the experiment to be on the order of a few hundred kHz (for SHMS singles), a few hundred Hz (for HMS singles) and on the order of a few Hz for the coincidence trigger rates.

p_m (MeV/c)	θ_{nq} (deg)	data-taking (hrs)	overhead (hrs)
500	70	24	2
800	49	200	2
	60	144	2
	72	160	2
$^1\text{H}(e, e'p)$ elastic		8	
target boiling		2	
BCM calibration		2	
total		540	8
			548 hrs (23 PAC days)

Table 4: Beam time allocation.

5 Summary

In summary, this proposal aims to measure for the first time the angular (θ_{nq}) distributions of the FSI/PWIA cross-section ratios for the exclusive $d(e, e'p)n$ reaction at large momentum transfers ($Q^2 = 4.5 \text{ GeV}/c^2$) and very high missing momenta ($p_m \sim 800 \text{ MeV}/c$) which corresponds to a kinematic region where the non-nucleonic components of the deuteron are expected to become relevant [15].

The previous $d(e, e'p)$ commissioning experiment [14] at Hall C extended the missing momentum reach up to $940 \text{ MeV}/c$ optimized for kinematics with reduced FSI at forward angles $\theta_{nq} \sim 40^\circ$. The unexpected results of that experiment, particularly starting at $p_m \sim 750 \text{ MeV}/c$, coincides with the expected inelastic transition within the deuteron [15]. This observation has reinvigorated a theoretical as well as experimental interest in studying the repulsive core of this simple nucleus.

The main objective of this proposal is therefore to focus on extracting the FSI/PWIA angular distributions to more precisely pin down the behavior of final-state interactions at very high missing momenta while covering a wide range of neutron recoil angles to map out the angular distributions and be able to definitively rule out any possible contributions from FSI in the kinematic region corresponding to the repulsive core of the deuteron.

References

- [1] W. Boeglin and M. Sargsian, *Modern studies of the Deuteron: From the lab frame to the light front*, *International Journal of Modern Physics E* **24** (2015) 1530003, [<https://doi.org/10.1142/S0218301315300039>].
- [2] L. L. Frankfurt, W. R. Greenberg, G. A. Miller, M. M. Sargsian and M. I. Strikman, *Color transparency effects in electron deuteron interactions at intermediate Q^{*2}* , *Z. Phys. A* **352** (1995) 97–113, [[nucl-th/9501009](#)].
- [3] L. L. Frankfurt, M. M. Sargsian and M. I. Strikman, *Feynman graphs and generalized eikonal approach to high energy knock-out processes*, *Phys. Rev. C* **56** (Aug, 1997) 1124–1137.
- [4] M. M. Sargsian, *Selected Topics in High Energy Semi-Exclusive Electro-Nuclear Reactions*, *International Journal of Modern Physics E* **10** (Dec, 2001) 405–457.
- [5] C. Ciofi degli Atti and L. P. Kaptari, *Calculations of the exclusive processes $H-2(e, e\text{-prime } p)n$, $He-3(e, e\text{-prime } p)H-2$ and $He-3(e, e\text{-prime } p)(pn)$ within a generalized Glauber approach*, *Phys. Rev. C* **71** (2005) 024005, [[nucl-th/0407024](#)].
- [6] J. Laget, *The electro-disintegration of few body systems revisited*, *Physics Letters B* **609** (2005) 49 – 56.
- [7] S. Jeschonnek and J. W. Van Orden, *New calculation for $^2H(e, e'p)n$ at gev energies*, *Phys. Rev. C* **78** (Jul, 2008) 014007.
- [8] M. M. Sargsian, *Large Q^2 electrodisintegration of the deuteron in the virtual nucleon approximation*, *Phys. Rev. C* **82** (Jul, 2010) 014612.
- [9] W. P. Ford, S. Jeschonnek and J. W. Van Orden, *$^2H(e, e'p)$ observables using a Regge model parameterization of final state interactions*, *Phys. Rev. C* **87** (2013) 054006, [[1304.0647](#)].
- [10] R. J. Glauber, *Cross sections in deuterium at high energies*, *Phys. Rev.* **100** (Oct, 1955) 242–248.
- [11] R. J. Glauber, *Lectures in Theoretical Physics Volume 1*, .
- [12] FOR THE HALL A COLLABORATION collaboration, W. U. Boeglin, L. Coman, P. Ambrozewicz, K. Aniol, J. Arrington, G. Batigne et al., *Probing the high momentum component of the deuteron at high Q^2* , *Phys. Rev. Lett.* **107** (Dec, 2011) 262501.
- [13] CLAS COLLABORATION collaboration, K. S. Egiyan, G. Asryan, N. Gevorgyan, K. A. Griffioen, J. M. Laget, S. E. Kuhn et al., *Experimental Study of Exclusive $^2H(e, e'p)n$ Reaction Mechanisms at High Q^2* , *Phys. Rev. Lett.* **98** (Jun, 2007) 262502.
- [14] HALL C COLLABORATION collaboration, C. Yero, D. Abrams, Z. Ahmed, A. Ahmidouch, B. Aljawrneh, S. Alsalmi et al., *Probing the deuteron at very large internal momenta*, *Phys. Rev. Lett.* **125** (Dec, 2020) 262501.

- [15] M. M. Sargsian and F. Vera, *New structure in the deuteron*, *Phys. Rev. Lett.* **130** (Mar, 2023) 112502.
- [16] F. Vera, *Probing the Structure of Deuteron at Very Short Distances*. Phd thesis, Florida International University, Miami, FL, July, 2021.
- [17] T. D. Forest, *Off-shell electron-nucleon cross sections: The impulse approximation*, *Nuclear Physics A* **392** (1983) 232–248.
- [18] W. U. Boeglin. Private communication, October, 2019.
- [19] C. Yero, *Cross Section Measurements of Deuteron Electro-Disintegration at Very High Recoil Momenta and Large 4-Momentum Transfers (Q^2)*. Phd thesis, Florida International University, Miami, FL, July, 2020.
- [20] L. L. Frankfurt, M. M. Sargsian and M. I. Strikman, *Feynman graphs and Gribov-Glauber approach to high-energy knockout processes*, *Phys. Rev. C* **56** (1997) 1124–1137, [[nucl-th/9603018](#)].

6 Appendix

6.1 PAC 52: LOI 12-24-005 || Reader Comments

The main goal of the LOI is to study the repulsive core of the short-range neutron-proton correlation inside deuterium. To this aim, the main problem is to find a kinematics where all other possible effects, in particular FSI, are suppressed.

Both theory expectations (Fig.1), previous experimental results (Fig.2), and your simulations of Fig.12 (**Fig.13 in PAC 53 proposal**) deliver the same message that the peak of FSI effects shifts to lower recoiling-neutron angles θ_{nq} at increasing missing momentum p_{miss} . The results in Fig.3 from previous Hall A experiment seem consistent: if the peak FSI shifts at lower θ_{nq} at larger p_{miss} , then the larger θ_{nq} the earlier (= the smaller p_{miss}) for the onset of FSI. Indeed, Fig.3 shows solid curves (FSI) that deviate from dashed ones (PWIA) for p_{miss} well below 700 MeV/c, even at 500 MeV/c at the largest angle (rightmost plot).

However, the puzzling feature of Fig.3 is that starting from some p_{miss} theory calculations (with or without FSI) start deviating from data. In the LOI, emphasis is put on the results for the CD Bonn optical potential, which deviate from data at very large $p_{miss} > 700$ -800 MeV/c, depending on the angle. I understand that the reason for this emphasis is that at these p_{miss} there is the inelastic threshold of proton-neutron channel, opening up non-nucleonic degrees of freedom.

But results from other optical potential show very different deviations, even at p_{miss} as low as 500 MeV/c (green and blue curves in the leftmost plot). All the calculations (optical potential, off-shell electron-nucleon cross section in Eq.(4)) are all done in a non-relativistic framework, which is definitely not adequate for $p_{miss} \sim 800$ MeV/c which is the focus of the LOI. Moreover, relativistic corrections could heavily modify the simulations in Fig.12 (**Fig.13 in PAC 53 proposal**) for the largest p_{miss} values.

So, why invoking "exotic" effects (".. possible indication of the onset of non-nucleonic degrees of freedom...") before having all relativistic corrections under control?

I have also another question. In all previous experiments, and in the simulation discussed in Fig.12 (**Fig.13 in PAC 53 proposal**), there seems to be a specific angle, $\theta_{nq} \sim 40$ deg, at which FSI "switch off", irrespective of the kinematics explored (small or large p_{miss} , it does not matter). Since the indication instead is for a peak of FSI over PWIA shifting with p_{miss} , I'm wondering if there is any special reason for this 40 deg. angle. If there were one, it could solve the main problem raised in the LOI (= switch off FSI) without any additional measurement...

6.1.1 Question:

So, why invoking "exotic" effects (".. possible indication of the onset of non-nucleonic degrees of freedom...") before having all relativistic corrections under control?

Response:

We agree that one should expect significant relativistic effects for momenta above ~ 800 MeV/c, without attributing it to exotic non-nucleon component in the deuteron. However, as it was predicted in Ref. [15] the existence of non-nucleon components above the pn threshold will result in a violation of so-called "angular condition", in which case the extracted light-cone momentum distribution of the deuteron will depend on light cone momentum k and its transverse component k_{\perp} independently. Or in other words the non-polarized momentum distribution will depend on the direction of the internal momentum of the deuteron on the light-front. Even for the most relativistic case, if deuteron consists of proton and neutron only, the angular condition is satisfied and light-cone momentum distribution depends on the magnitude of k only. However, the existence of non-nucleonic component in the deuteron will result in an angular anisotropy [15]. Thus to obtain the signature of non-nucleon component the experiment needs to isolate the light-cone momentum distribution of the deuteron without effects of final-state interaction. As a result, exploring the possible onset of non-nucleonic degrees of freedom in the deuteron requires a solid understanding of final-state interactions at bound nucleon momenta above ~ 800 MeV/c.

As such this proposal does **not** focus on searching for non-nucleonic components, but rather focuses on investigating the angular dependence of final-state interactions with θ_{nq} at momenta where non-nucleonic effects are expected to emerge in the ground state of deuteron wave function, i.e., ~ 800 MeV/c, (above the inelastic threshold of pn system) as there is currently **no** data that explores FSI in this region.

6.1.2 Question:

In all previous experiments, and in the simulation discussed in Fig.12(Fig.13 in PAC 53 proposal), there seems to be a specific angle, $\theta_{nq} \sim 40$ deg, at which FSI "switch off", irrespective of the kinematics explored (small or large p_{miss} , it does not matter). Since the indication instead is for a peak of FSI over PWIA shifting with p_{miss} , I'm wondering if there is any special reason for this 40 deg. angle. If there were one, it could solve the main problem raised in the LOI (= switch off FSI) without any additional measurement...

Response:

Experimentally, there is **no** angle at which FSI are "turn off". The mention of a specific angle $\theta_{nq} \sim 40^\circ$ just refers the central value of a broader angular region at which FSI are suppressed. There are only certain angular regions in which FSI are the dominant contribution to the $d(e, e'p)n$ cross-section, and there are other regions in which FSI are suppressed, mainly at forward ($\theta_{nq} \lesssim 40^\circ$) and backward ($\theta_{nq} \gtrsim 120^\circ$) angles. At backward angles, the kinematics are inelastic ($x_{Bj} < 1$) and intermediate nucleonic excitations like

Isobar contributions contribute significantly to the cross-section, whereas at forward angles, $x_{Bj} > 1$, the PWIA becomes the dominant contribution to the $d(e, e'p)n$ cross-section.

The suppression of FSI at $\theta_{nq} \sim 40^\circ$ is due to cancellation of PWIA-FSI interference term with the $|FSI|^2$ term. This is a feature of eikonal (high energy) regime of FSI in which case pn rescattering amplitude is mainly imaginary and as a result Real part of the $iA_{FSI}A_{PWIA}$ interference term is negative, cancelling the $|A_{FSI}|^2$ term. As a result of this cancellation the cross section in this case is dominated by $|A_{PWIA}|^2$ term. This cancellation is in a fairly broad range of θ_{nq} and p_m . It was investigated in Ref. [1] within generalized eikonal approximation (GEA) and has been found that its position is defined by the average characteristics of the deuteron, pn re-scattering amplitude and kinetic energy of recoil particle. In the most simplified version (assuming single exponential form of the deuteron wave function) the cancellation happens at the transverse momentum of recoil nucleon:

$$p_{r\perp} \sim \sqrt{\frac{1}{\alpha_d} \ln \frac{32\pi\alpha_d}{\sigma_{pn}} + \frac{B_{pn}M_N^2}{2}\Delta^2},$$

where σ_{pn} is the total cross section of pn scattering, $\alpha_d = \frac{r_{rms}}{2p_{rms}}$, where r_{rms} and p_{rms} are RMS values of deuteron radius and internal momentum, B_{pn} is the exponent of the pn scattering amplitude presented in the diffractive form, M_N - is the mass of the nucleon, and $\Delta = \frac{q_0}{q}T_r$ where T_r , q_0 and q are the kinetic energy of the recoil nucleon, energy and momentum of the virtual photon respectively. Note that the Δ term accounts for the non-zero momentum of the of the scatterer in the deuteron which is not accounted in the standard Glauber approximation [20].

It is important to note that the angular dependence of the cross-sections on FSI has only been measured for recoil neutron momenta up to ~ 500 MeV/c [12], and predictions made about the suppression of FSI above ~ 500 MeV/c can be checked in the proposed experiment.